

Molecular Structure of an Fe(IV) Species: $\{[\text{Fe}(\text{TTP})]_2\text{N}\}\text{SbCl}_6$ Ming Li,[†] Maoyu Shang,[†] Noelle Ehlinger,[†] Charles E. Schulz,^{*,‡} and W. Robert Scheidt^{*,‡}

The Department of Chemistry and Biochemistry, University of Notre Dame, Notre Dame, Indiana 46556, and The Department of Physics, Knox College, Galesburg, Illinois 61401

Received July 29, 1999

The molecular structure of the formal iron(IV) porphyrinate derivative, $\{[\text{Fe}(\text{TTP})]_2\text{N}\}\text{SbCl}_6$ (TTP = tetratolylporphyrinate), is reported. The structural parameters are compared to the previously reported species $[\text{Fe}(\text{TPP})]_2\text{N}$, in which the iron oxidation state is +3.5. Both the equatorial and axial bond distances in $\{[\text{Fe}(\text{TTP})]_2\text{N}\}\text{SbCl}_6$ are slightly shortened and consistent with an increased formal charge on iron. The value for the axial Fe–N distance is 1.6280(7) Å, and the average value of the equatorial Fe–N_p distances is 1.979(5) Å. The Mössbauer isomer shift decreases upon oxidation, again consistent with an increase in formal charge. Values for the isomer shift at room temperature are –0.13 mm/s for $\{[\text{Fe}(\text{TTP})]_2\text{N}\}\text{SbCl}_6$ and 0.04 mm/s for $[\text{Fe}(\text{TPP})]_2\text{N}$. Crystal data for $\{[\text{Fe}(\text{TTP})]_2\text{N}\}\text{SbCl}_6$ are as follows: orthorhombic, space group *Fddd*, *Z* = 8, *a* = 23.689(2) Å, *b* = 31.056(3) Å, *c* = 22.7788(18) Å.

Introduction

Highly oxidized porphyrin complexes have been proposed as intermediates in a number of heme proteins, including catalase,¹ peroxidase,² and cytochrome P-450.³ Because of the unusual electronic properties and the novel reactivities that these intermediates demonstrate, there is current interest in the preparation and characterization of synthetic analogues of (porphyrinato)iron complexes oxidized beyond the Fe(III) state.^{4–7} One of the first such higher-oxidation-state porphyrin species prepared was $[\text{Fe}(\text{TPP})]_2\text{N}$.^{8,9} These dinuclear μ -nitridodiiron complexes have been characterized by XPS,¹⁰ by Mössbauer,^{9,11} EPR,¹² and resonance Raman spectroscopies;¹³

and by determination of molecular structures.¹⁴ The species contain a symmetric, linear $[\text{Fe}=\text{N}=\text{Fe}]^{4+}$ moiety, in which both iron ions are formally in the oxidation state +3.5. These complexes can be electrochemically and chemically oxidized to yield the Fe(IV) species based on Mössbauer spectra¹⁵ but have not yet been structurally characterized.

There have been several structurally characterized examples of iron(IV) complexes that utilize phthalocyanine or octaethylcorrole (H₃OEC) macrocycles. Examples include $[(\text{N}_3)(\text{Pc})\text{Fe}-\text{N}-\text{Fe}(\text{Pc})(\text{N}_3)]^-$,¹⁶ $[(\text{THF})(\text{TPP})\text{Fe}-\text{N}-\text{Fe}(\text{Pc})(\text{H}_2\text{O})]^+$,¹⁷ $[\text{Fe}(\text{Pc})(\text{Br})]_2\text{N}$,¹⁸ $[\text{Fe}(\text{OEC})(\text{Cl})]$,¹⁹ and $[\text{Fe}^{\text{IV}}(\text{OEC}\cdot)\text{C}_6\text{H}_5]^+$.²⁰ In addition, Fe(IV) complexes with a tetraamido macrocycle, H₄[MAC*], have been characterized by the Collins' group.^{21,22} In the present work, we report the X-ray structure determination and infrared spectrum of $\{[\text{Fe}(\text{TTP})]_2\text{N}\}\text{SbCl}_6$. The structural information for this iron(IV) species is compared with that of neutral $[\text{Fe}(\text{TPP})]_2\text{N}$ and analogous complexes.

Experimental Section

General Information. All manipulations were carried out under argon using a double manifold vacuum line, Schlenkware, and cannula techniques. Dichloromethane was distilled over CaH₂, and hexanes were distilled over sodium benzophenone. All other chemicals were used as

* To whom correspondence should be addressed.

† University of Notre Dame.

‡ Knox College.

- Reid, T. V.; Murthy, M. R. N.; Sicignano, A.; Tanaka, N.; Musick, W. D. L.; Rossman, M. G. *Proc. Natl. Acad. Sci. U.S.A.* **1981**, *78*, 4767.
- Hewson, W. D.; Hager, L. P. In *Porphyrins*; Dolphin, D., Ed.; Academic Press: New York, Vol. 7, pp 295–332.
- Groves, J. T.; Han, Y.-Z. In *Cytochrome P-450. Structure, Mechanism and Biochemistry*; Ortiz de Montellano, P. R., Ed.; Plenum Press: New York, 1995; pp 3–48.
- Czarnecki, K.; Nimri, S.; Gross, Z.; Proniewicz, Z. M.; Kincaid, J. R. *J. Am. Chem. Soc.* **1996**, *118*, 2929.
- Hickman, D. L.; Nanthakumar, A.; Goff, H. M. *J. Am. Chem. Soc.* **1988**, *110*, 6384.
- Groves, J. T.; Gross, Z.; Stern, M. K. *Inorg. Chem.* **1994**, *33*, 5056.
- Simonneaux, G.; Sholz, W. F.; Reed, C. A.; Lang, G. *Biochim. Biophys. Acta* **1982**, *716*, 1.
- Abbreviations: XPS, X-ray photoelectron spectroscopy; TPP, tetraphenylporphyrinato anion; TTP, tetratolylporphyrinato anion; N_p, porphyrinato nitrogen atom; Pc, phthalocyaninato anion; OEP, octethylporphyrinato anion; THF, tetrahydrofuran, H₄ [MAC*], 1, 4, 8, 11-tetraaza-13, 13-diethyl-2, 2, 5, 5, 7, 7, 10, 10-octamethyl-3, 6, 9, 12, 14-pentaoxocyclotetradecane.
- Summerville, D. A.; Cohen, I. A. *J. Am. Chem. Soc.* **1976**, *98*, 1747.
- Kadish, K. M.; Bottomley, L. A.; Brace, J. G.; Winograd, N. *J. Am. Chem. Soc.* **1980**, *102*, 4341.
- Ercolani, C.; Hewage, S.; Heucher, R.; Rossi, G. *Inorg. Chem.* **1993**, *32*, 2975.
- Bocian, D. F.; Findsen, E. W.; Hofmann, J. A.; Schick, G. A.; English, D. R.; Hendrickson, D. N.; Suslick, K. S. *Inorg. Chem.* **1984**, *23*, 800.
- Schick, G. A.; Bocian, D. F. *J. Am. Chem. Soc.* **1983**, *105*, 1830.

- Scheidt, W. R.; Summerville, D. A.; Cohen, I. A. *J. Am. Chem. Soc.* **1976**, *98*, 6623.
- (a) English, D. R.; Hendrickson, D. N.; Suslick, K. S. *Inorg. Chem.* **1983**, *22*, 367. (b) English, D. R.; Hendrickson, D. N.; Suslick, K. S. *Inorg. Chem.* **1985**, *24*, 122.
- Kienast, A.; Homborg, H. Z. *Anorg. Allg. Chem.* **1998**, *624*, 233.
- Ercolani, C.; Jubb, J.; Pennesi, G.; Russo, U.; Trigiant, G. *Inorg. Chem.* **1995**, *34*, 2535.
- Moubaraki, B.; Benlian, D.; Baldy, A.; Pierrot, M. *Acta Crystallogr., Sect. C* **1989**, *C45*, 393.
- Vogel, E.; Will, S.; Schulze, T. A.; Neumann, L.; Lex, J.; Bill, E.; Trautwein, A. X.; Wieghardt, K. *Angew. Chem., Int. Ed. Engl.* **1994**, *33*, 731.
- Caemelbecke, E. V.; Will, S.; Autret, M.; Adamian, V. A.; Lex, J.; Gisselbrecht, J.-P.; Gross, M.; Vogel, E.; Kadish, K. M. *Inorg. Chem.* **1996**, *35*, 184.
- Kostka, K. L.; Fox, B. G.; Hendrich, M. P.; Collins, T. J.; Rickard, C. E. F.; Wright, L. J.; Munck, E. *J. Am. Chem. Soc.* **1993**, *115*, 6746.
- Collins, T. J.; Fox, B. G.; Hu, Z. G.; Kostka, K. L.; Munck, E.; Rickard, C. E. F.; Wright, L. J. *J. Am. Chem. Soc.* **1992**, *114*, 8724.

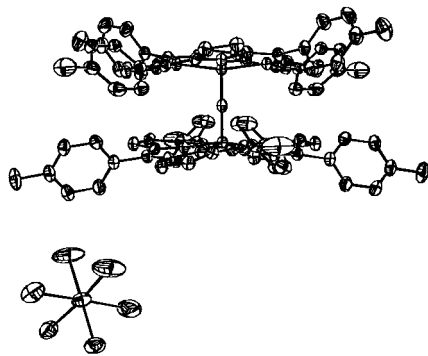


Figure 1. ORTEP diagrams of the structure $\{[\text{Fe}(\text{TTP})_2]_2\text{N}\}\text{SbCl}_6$. Thermal ellipsoids of atoms are contoured at the 50% probability level. Hydrogen atoms have been omitted for clarity. Only one position of the disordered $[\text{SbCl}_6]^-$ anion is shown.

Table 1. Crystallographic Details

formula	$\text{C}_{96}\text{H}_{72}\text{Cl}_6\text{Fe}_2\text{N}_9\text{Sb}\cdot\text{CH}_2\text{Cl}_2$
FW, amu	1882.70
a , Å	23.689(2)
b , Å	31.056(3)
c , Å	22.7788(18)
V , Å ³	16758(2)
space group	$Fddd$
Z	8
D_c , g/cm ³	1.492
$F(000)$	7664
μ , mm ⁻¹	0.972
crystal dimensions, mm	0.30 × 0.12 × 0.10
radiation	Mo $K\alpha$, $\lambda = 0.71073$ Å
goodness-of-fit (based on F^2)	1.068
final R indices [$I > 2\sigma(I)$]	$R_1 = 0.0702$, $wR_2 = 0.1367$
final R indices (all data)	$R_1 = 0.1092$, $wR_2 = 0.1538$

received from Aldrich or Fisher. $[\text{Fe}(\text{TTP})\text{Cl}]$ and $[\text{Fe}(\text{TTP})\text{N}_3]$ were synthesized by literature methods.^{23,24} UV-vis spectra were recorded on a Perkin-Elmer Lambda 19 spectrometer and IR spectra on a Perkin-Elmer model 883 as KBr pellets. EPR spectra were obtained at 77 K on a Varian E-12 spectrometer operating at X-band. The solid-state Mössbauer samples were immobilized in Apiezon grease in a zero field.

Synthesis of μ -Nitrido-bis(5,10,15,20-tetratolylporphyrinato)-iron. $[\text{Fe}(\text{TTP})_2]\text{N}$ was prepared by the method of Summerville and Cohen.⁹ UV-vis (CH_2Cl_2 solution) λ_{max} (log ϵ): 386 (5.35), 410 (5.35), 534 (4.56), 625 (4.38) nm. IR(KBr): ν (Fe-N-Fe) 910(s), 884(m) cm^{-1} . EPR (frozen CH_2Cl_2 , 77K) $g_{\perp} = 2.14$, $g_{\parallel} = 2.01$.

Preparation of $\{[\text{Fe}(\text{TTP})_2]\text{N}\}\text{SbCl}_6$. $[\text{Fe}(\text{TTP})_2]\text{N}$ (20 mg, 0.017 mmol) and tris(*p*-bromophenyl)ammonium hexachloroantimonate (17 mg, 0.020 mmol) were placed in a 100 mL Schlenk flask, and dichloromethane (~20 mL) was added. The solution was stirred for 1 h and transferred into two 10-mL beakers which were inside crystallizing bottles; the bottles were then placed in a refrigerator (4 °C). Hexane was used to induce crystallization by slow vapor diffusion. Dark-purple crystals formed after ~5 days. UV-vis, IR, and Mössbauer spectra were measured on samples comprised of selected crystals. UV-vis (CH_2Cl_2 solution) λ_{max} (log ϵ): 398 (5.18), 534 (4.03) nm. IR(KBr): ν (Sb-Cl) 343 cm^{-1} .

X-ray Structure Determination of $\{[\text{Fe}(\text{TTP})_2]\text{N}\}\text{SbCl}_6$. Single-crystal experiments were carried out on a Nonius FAST area-detector diffractometer with a Mo rotating anode source ($\lambda = 0.71073$ Å). Our detailed methods and procedures for small molecular X-ray data collection have been described previously.²⁵ A total of 26 164 reflections were collected, of which 4920 were unique, and intensities of 3487 unique reflections were larger than $2\sigma(I)$. All reflections were reduced

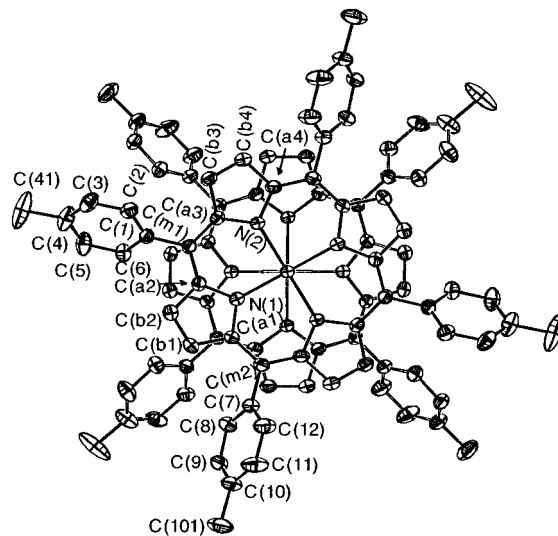


Figure 2. Topview of $\{[\text{Fe}(\text{TTP})_2]_2\text{N}\}^+$. Thermal ellipsoids of atoms are contoured at the 50% probability level.

Table 2. Comparison of Average Distances (Å) and Angles (deg) for the μ -Nitrido Species^a

	$\{[\text{Fe}(\text{TTP})_2]_2\text{N}\}\text{SbCl}_6$	$[\text{Fe}(\text{TPP})_2]\text{N}$
Fe-N _p	1.979(5)	1.991(3)
Fe-N _{ax}	1.6280(7)	1.661(7)
N _p -C _a	1.384(4)	1.381(5)
C _b -C _b	1.347(3)	1.348(9)
C _a -C _b	1.429(4)	1.434(2)
C _a -C _m	1.385(4)	1.387(8)
C _m -C _{ph}	1.492(5)	1.495(5)
N _p -Fe-N _p	88.7(9)	88.7(3)
Fe-N-C _a	127.0(8)	127.0(10)
C _a -N-C _a	105.0(3)	105.6(3)
N-C _a -C _b	110.2(3)	110.0(4)
N-C _a -C _m	125.2(5)	125.5(3)
C _a -C _b -C _b	107.2(3)	107.2(3)
C _a -C _m -C _a	122.5(8)	122.7(6)
C _b -C _a -C _m	124.4(4)	124.4(3)

^a The numbers in parentheses are the esd's of the average.

using Lorentz-polarization factors. The structure of $\{[\text{Fe}(\text{TTP})_2]\text{N}\}\text{SbCl}_6$ was solved by direct methods. The SbCl_6^- ion and its neighboring CH_2Cl_2 solvent molecules were disordered around an intersection of three 2-fold axes (see Figure S1). After all non-hydrogen atoms were refined to converge anisotropically,²⁶ a difference Fourier map showed most of the hydrogen atoms. However, these hydrogen atoms were included in the final refinement only as idealized riding atoms along with the remaining hydrogen atoms, whose positional parameters were generated theoretically (C-H = 0.95 Å). The structure was refined against F^2 by the SHELXL-93 program.²⁷ The refinement converged to final values of $R_1 = 0.0702$ and $wR_2 = 0.1367$ for observed unique reflections ($I > 2\sigma(I)$) and $R_1 = 0.1092$, $wR_2 = 0.1538$ for all unique reflections, including those with negative intensities. The weighted R factors, wR , are based on F^2 and conventional R factors, R , on F , with F set to zero for negative intensities. All reflections, including those with negative intensities, were included in the refinement, and the $I > 2\sigma(I)$ criterion was used only for calculating R_1 . The maximum and minimum residual electron densities on the final difference Fourier map were 0.38 and 0.66 $e/\text{Å}^3$, respectively. A brief summary of determined parameters is listed in Table 1.

Results and Discussion

The X-ray structure of the one-electron oxidation product of $[\text{Fe}(\text{TTP})_2]\text{N}$ was determined. ORTEP diagrams of the

(23) Adler, A. D.; Longo, F. R.; Kampas, F.; Kim, J. *J. Inorg. Nucl. Chem.* **1970**, *32*, 2443.

(24) Byers, W.; Cossham, J. A.; Edwards, J. O.; Gordon, A. T.; Jones, J. G.; Kenny, E. T. P.; Mahmood, A.; McKnight, J.; Sweigart, D. A.; Tondreau, G. A.; Wright, T. *Inorg. Chem.* **1986**, *25*, 4767.

(25) Scheidt, W. R.; Turowska-Tyrk, I. *Inorg. Chem.* **1994**, *33*, 1314.

(26) Sheldrick, G. M. *Acta Crystallogr.* **1990**, *A46*, 467.

(27) Sheldrick, G. M. *J. Appl. Crystallogr.*, in preparation.

Table 3. Selected Structural Features for Monobridged Binuclear Porphinato Complexes

compound	Fe–N _p , ^a Å	Fe–Y, ^b Å	Fe–Y–Fe, deg	Δ, ^c Å	Δ(N _p), ^d Å	mean plane sepn, ^e Å	interplanar angle, ^f deg	twist angle, ^g deg	ref
{[Fe(TTP)] ₂ N}SbCl ₆	1.979(5)	1.6280(7)	180	0.37	0.34	4.00	0.0	30.3	this work
[Fe(TPP)] ₂ N	1.991(3)	1.661(7)	180	0.41	0.32	4.15	0.0	31.7	14
[Fe(TPP)] ₂ C	1.980(8)	1.675	180		0.26	3.87	0.0	31.7	30
[Fe(OEP)] ₂ C	1.986(5)	1.6638(9)	179.5		0.19			21.0	31
[Fe(TPP)] ₂ O	2.087(3)	1.763(1)	174.5(1)	0.54	0.50	4.58	3.7	35.4	32

^a N_p refers to the pyrrole nitrogen atom in the porphyrin ring. ^b Y is the bridging atom. ^c The average displacement of the metal centers from the mean 24-atom core. A positive value indicates that the metal is displaced toward ring center. ^d 4-nitrogen atom plane. ^e The average separation of the individual atom from the other 24-atom core is given. ^f The dihedral angle of two mean planes of the 24-atom core within a dimeric molecule. ^g Average of the four N–M–M'–N' dihedral angles.

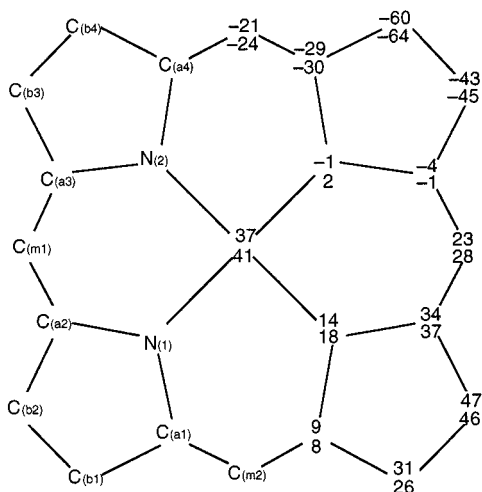


Figure 3. Formal diagram of the porphinato core of {[Fe(TTP)]₂N}⁺ and [Fe(TPP)]₂N displaying values of the perpendicular displacements of each atom (in units of 0.01 Å) from the mean plane of the 24-atom porphyrinato core; the upper value of the pair is that for {[Fe(TTP)]₂N}⁺, whereas the lower value is that for [Fe(TPP)]₂N. A positive value is a displacement toward the bridging nitrogen atom.

{[Fe(TTP)]₂N}⁺ unit are shown in Figures 1 and 2. The presence of the hexachloroantimonate anion clearly indicates that {[Fe(TTP)]₂N}⁺ is a cation. All physical data are consistent with the metals as the site of oxidation. The infrared spectrum of {[Fe(TTP)]₂N}SbCl₆ (KBr pellet) shows no major bands in the 1270–1290 cm⁻¹ region; a strong absorption in this region has been associated with π-cation radical character in a variety of metallotetraarylporphyrin complexes.²⁸ The absence of these bands and the very intense band at 910 cm⁻¹ (assigned as asymmetric ν_{Fe–N–Fe}) are consistent with the hypothesis that the oxidation of [Fe(TTP)]₂N occurs at the metals rather than at the porphyrin rings. Although an EPR spectrum is observed for the nitrido bridged species, upon oxidation the complex becomes EPR-silent. Further support for this comes from Mössbauer spectra. The isomer shift value at room temperature (–0.13 mm/s) in {[Fe(TTP)]₂N}SbCl₆ is much lower than that observed in [Fe(TTP)]₂N (0.04 mm/s) and is in the range expected for an iron(IV) species.²⁹ Further, the quadrupole splitting values are 2.04 and 1.15 mm/s for {[Fe(TTP)]₂N}SbCl₆ and [Fe(TTP)]₂N, respectively. These observations are definitely consistent with an increased oxidation state for iron in {[Fe(TTP)]₂N}SbCl₆.

The structural differences between [Fe(TPP)]₂N and the {[Fe(TTP)]₂N}⁺ cation are also consistent with an increased formal charge on iron in the latter. The two iron centers in both

complexes are crystallographically equivalent with only one-fourth of the molecule unique. In {[Fe(TTP)]₂N}⁺, the two unique Fe–N_p bond distances are 1.974(3) and 1.983(3) Å, whereas the corresponding distances in neutral [Fe(TPP)]₂N are 1.990(3) and 1.992(3) Å.¹⁴ The former are significantly shorter than the latter but are almost identical to the distances found in the isoelectronic species [Fe(TPP)]₂C,³⁰ which are 1.974 and 1.986 Å. Another important difference between the neutral and cationic complexes is that the bridging Fe–N distance of 1.6280(7) Å in {[Fe(TTP)]₂N}SbCl₆ is considerably shorter than the 1.661(7) Å Fe–N distance observed in [Fe(TPP)]₂N. The required crystallographic symmetry in the two nitrido bridged species means that the Fe–N–Fe unit is required to be exactly linear in both derivatives. Although a direct comparison of an oxidized TPP derivative would clearly be desirable, we were unable to obtain acceptable crystals of {[Fe(TTP)]₂N}SbCl₆.

Table 2 compares the average bond distances and angles of several chemical classes in {[Fe(TTP)]₂N}SbCl₆ and [Fe(TPP)]₂N; complete bond distance and angle tabulations for {[Fe(TTP)]₂N}SbCl₆ are given in the Supporting Information. It should be noted that all bond lengths and angles in the porphyrin skeleton are effectively identical in the two derivatives. Differences are seen only in the Fe–N_p and Fe–N_{ax} distances of the two coordination groups. Thus, the structural features are convincing evidence for metal-centered oxidation and argue against the presence of porphyrin π-cation radical formation.

Figure 3 shows the perpendicular displacements of each atom from the mean plane of the 24-atom core for the two μ-nitrido species, {[Fe(TTP)]₂N}SbCl₆ (top) and [Fe(TPP)]₂N (bottom). The core conformation in the {[Fe(TTP)]₂N}⁺ cation is slightly less saddled than that in [Fe(TPP)]₂N. The displacement of the iron atoms is clearly a response to the steric effects of bringing the two porphyrin rings of the binuclear species in close proximity. In both nitrido derivatives, the displacement of the iron atom from the mean plane of the four nitrogen atoms is significantly smaller (Table 3) than that from the 24-atom mean plane. Although domed porphinato cores might be expected to better alleviate core interactions, the saddling in both complexes is the apparent result of the necessity of maintaining short Fe–N_p bonds. Also given in Table 3 are values for other single-atom bridged metalloporphyrins. Saddled cores are observed in all derivatives except the high-spin μ-oxo complex with its much longer Fe–N_p bonds and large out-of-plane displacement.

The separation between the two porphyrin mean planes in [Fe(TTP)]₂N}SbCl₆ is 4.00 Å, distinctly shorter than that found in [Fe(TPP)]₂N, as shown in Table 3. The decreased interplanar spacing leads to relatively small dihedral angles between the plane of the porphinato core and the two structurally unique

(28) Shimomura, E. T.; Phillippi, M. A.; Goff, H. M.; Scholz, W. F.; Reed, C. A. *J. Am. Chem. Soc.* **1981**, *103*, 6778.

(29) Debrunner, P. G. In *Iron Porphyrins*; Lever, A. B. P., Gray, H. B., Eds.; VCH Publishers Inc.: New York, 1989; Vol. 3, pp 139–227.

(30) Goedken, V. L.; Deakin, M. D.; Bottomley, L. A. *J. Chem. Soc., Chem. Commun.* **1982**, 607.

phenyl groups (53.4 and 60.0°). As was noted previously,³³ there is a correlation between the phenyl ring–phenyl ring orientation and the phenyl center–center distance for the closest phenyl groups on each porphyrin ring of the dimer. Thus, as the center–center distance between a pair of phenyl rings becomes smaller, the two rings adopt a geometry in which they become nearly perpendicular in order to minimize the phenyl–phenyl non-bonded interaction. In accord with this expectation, the phenyl center–center distance in {[Fe(TTP)]₂N}⁺ is 5.54 Å, and the Ph–Ph dihedral angle is 73.3°; the corresponding values are 5.77 Å and 65.3° in [Fe(TPP)]₂N, respectively.

Finally, we note that there are two Fe(IV) species with six-coordinate iron centers and smaller (but not zero) displacements of iron toward the bridging ligand. Some of the steric problems are alleviated by the presence of two different macrocycles. The iron displacements from the porphyrin ligand in [(THF)(TPP)-Fe–N–Fe(Pc)(H₂O)]⁺¹⁷ and [(THF)(TPP)Fe–C–FePc(THF)]³⁴ are both 0.12 Å (Δ (N_p)).

-
- (31) Kienast, A.; Galich, L.; Murray, K. S.; Moubaraki, B.; Lazarev, G.; Cashion, J.; Homborg, H. *J. Porphyrins Phthalocyanines* **1997**, *1*, 141.
(32) Hoffman, A. B.; Collins, D. M.; Day, V. W.; Fleischer, E. B.; Srivastava, T. S.; Hoard, J. L. *J. Am. Chem. Soc.* **1972**, *94*, 3620.
(33) Cheng, B.; Fries, P.; Marchon, J.; Scheidt, W. R. *Inorg. Chem.* **1996**, *35*, 1024.

Summary. We have reported the molecular structure of {[Fe(TTP)]₂N}SbCl₆. Compared to neutral [Fe(TPP)]₂N, the Fe–N_p and bridging Fe–N distances appear to change significantly. The EPR, Mössbauer and infrared spectra of {[Fe-(TTP)]₂N}SbCl₆ are in accord with the proposal that oxidation is centered in the iron atom rather than the porphyrin ring.

Acknowledgment. We thank the National Institutes of Health for support of this research under Grant GM-38401 to W.R.S. Funds for the purchase of the FAST area detector diffractometer was provided through NIH Grant RR-06709 to the University of Notre Dame.

Supporting Information Available: Tables S1–S6, giving complete crystallographic details, atomic coordinates, anisotropic temperature factors, fixed hydrogen atom positions, and complete listings of bond distances and angles for the complexes. Diagram showing disordered SbCl₆ counterion and CH₂Cl₂ (Figure S1). This material is available free of charge via the Internet at <http://pubs.acs.org>.

IC990900K

-
- (34) Galich, L.; Kienast, A.; Huckstadt, H.; Homborg, H. *Z. Anorg. Allg. Chem.* **1998**, *624*, 1235.